

## Chapter 3

### Lecture 10

#### Drag polar – 5

#### Topics

3.2.18 Parasite drag area and equivalent skin friction coefficient

3.2.19 A note on estimation of minimum drag coefficients of wings and bodies

3.2.20 Typical values of  $C_{D0}$ ,  $A$ ,  $e$  and subsonic drag polar

3.2.21 Winglets and their effect on induced drag

#### 3.3 Drag polar at high subsonic, transonic and supersonic speeds

3.3.1 Some aspects of supersonic flow - shock wave, expansion fan and bow shock

3.3.2 Drag at supersonic speeds

3.3.3 Transonic flow regime - critical Mach number and drag divergence Mach number of airfoils, wings and fuselage

#### 3.2.18 Parasite drag area and equivalent skin friction coefficient

As mentioned in remark (ii) of the previous subsection, the product  $C_{D0} \times S$  is called the parasite drag area. For a streamlined airplane the parasite drag is mostly skin friction drag. Further, the skin friction drag depends on the wetted area which is the area of surface in contact with the fluid. The wetted area of the entire airplane is denoted by  $S_{wet}$ . In this background the term 'Equivalent skin friction coefficient ( $C_{fe}$ )' is defined as:

$$C_{D0} \times S = C_{fe} \times S_{wet}$$

$$\text{Hence, } C_{fe} = C_{D0} \times \frac{S}{S_{wet}} \text{ and } C_{D0} = C_{fe} \frac{S_{wet}}{S} \quad (3.47)$$

Reference 3.9, Chapter 12 gives values of  $C_{fe}$  for different types of airplanes.

### Example 3. 3

A quick estimate of the drag polar of a subsonic airplane is presented in this example which is based Ref.3.7, section 14.8. However, modifications have been incorporated, keeping in view the present treatment of the drag polar.

An airplane has a wing of planform area  $51.22 \text{ m}^2$  and span  $20 \text{ m}$ . It has a fuselage of frontal area  $3.72 \text{ m}^2$  and two nacelles having a total frontal area of  $3.25 \text{ m}^2$ . The total planform area of horizontal and vertical tails is  $18.6 \text{ m}^2$ . Obtain a rough estimate of the drag polar in a flight at a speed of  $430 \text{ kmph}$  at sea level, when the landing gear is in retracted position.

#### Solution:

Flight speed is  $430 \text{ kmph} = 119.5 \text{ m/s}$ .

Average chord of wing ( $\bar{c}_{\text{wing}}$ ) =  $S / b = 51.22/20 = 2.566 \text{ m}$ .

The value of kinematic viscosity ( $\nu$ ) at sea level =  $14.6 \times 10^{-6} \text{ m}^2$

Reynolds number ( $R_e$ ) based on average chord is:

$$\frac{119.5 \times 2.566}{14.6 \times 10^{-6}} = 21 \times 10^6$$

It is assumed that NACA 23012 airfoil is used on the wing. From Ref.3.14, Appendix IV, the minimum drag coefficient,  $(C_d)_{\text{min}}$ , of this airfoil at  $Re = 9 \times 10^6$  is  $0.006$ . However, the value of drag coefficient is required at  $Re = 21 \times 10^6$ .

Assuming the flow to be turbulent  $(C_d)_{\text{min}}$  can be taken proportional to  $R_e^{-\frac{1}{7}}$  (Eq. 3.35). Thus,  $C_{d\text{min}}$  at  $Re_w = 21 \times 10^6$  would roughly be equal to:

$$0.006 \times (21 \times 10^6)^{-\frac{1}{7}} / (9 \times 10^6)^{-\frac{1}{7}} = 0.0053$$

As regards the fuselage and nacelle, the frontal areas are specified. Hence, they are treated as a bluff bodies. The value of  $(C_{D\text{min}})_{\text{fuselage}}$  can be taken as  $0.08$  (Ref.3.4). The nacelle generally has a lower fineness ratio and  $(C_{D\text{min}})_{\text{nac}}$  can be taken as  $0.10$ .

Flight dynamics-I  
Chapter-3

As regards the horizontal and vertical tails, the Reynolds number based on their average chords ( $Re_{tail}$ ) can be calculated if the areas and spans of these were given. The following is suggested to obtain a rough estimate of  $Re_{tail}$ .

$$S_{ht} \approx S_{vt} \approx 18.6/2 \approx 9.3 \text{ m}^2. \text{ Then}$$

$$\frac{\bar{c}_{tail}}{\bar{c}_{wing}} \approx \sqrt{\frac{S_{tail}}{S_{wing}}}$$

$$\text{and } \frac{Re_{tail}}{Re_w} \approx \frac{\bar{c}_{tail}}{\bar{c}_{wing}} \approx \sqrt{\frac{9.3}{51.22}} = 0.426$$

$$\text{Hence, } Re_{tail} \approx 21 \times 10^6 \times 0.426 = 8.95 \times 10^6 \approx 9 \times 10^6$$

At this Reynolds number ( $C_{dmin}$ )<sub>tail</sub> can be assumed to be 0.006

The calculation of the parasite drag coefficient ( $C_{D0}$ ) is presented in Table E 3.3.

Part	$S_{\pi}$ (m <sup>2</sup> )	$C_{D\pi}$	$C_{D\pi} S_{\pi}$ (m <sup>2</sup> )
Wing	51.22	0.0053	0.271
Fuselage	3.72	0.080	0.298
Nacelles	3.25	0.1	0.325
Tail surfaces	18.6	0.006	0.112
		Total	1.006

Table E3.3 Rough estimate of  $C_{D0}$

Adding 10% for interference effects, the total parasite drag area ( $C_{D\pi} S_{\pi}$ ) is:

$$1.006 + 0.1006 = 1.1066 \text{ m}^2.$$

$$\text{Hence, } C_{D0} = 1.1066/51.22 = 0.0216$$

$$\text{Wing aspect ratio is } 20^2 / 51.22 = 7.8$$

To obtain Oswald efficiency factor for the airplane ( $e$ ), the quantities  $e_{wing}$ ,  $e_{fuselage}$  and  $e_{other}$  are obtained below.

Equations (3.42) and (3.43) give :

Flight dynamics-I  
Chapter-3

$$e_{\text{Wing}} = \frac{1.1(C_{L\alpha W} / A)}{R\left(\frac{C_{L\alpha W}}{A}\right) + (1-R)\pi}$$

$$C_{L\alpha W} = \frac{2\pi A}{2 + \sqrt{\frac{A^2 \beta^2}{\kappa^2} \left(1 + \frac{\tan 2\Lambda_{\frac{1}{4}}}{\beta^2}\right)} + 4}$$

Here

$$A = 7.8, M = V/a = 119.5/340 = 0.351$$

$$\text{Hence, } \beta = \sqrt{1-M^2} = \sqrt{1-0.351^2} = 0.936$$

For the purpose of calculating  $e_{\text{wing}}$ , the taper ratio ( $\lambda$ ), the quarter chord sweep ( $\Lambda_{\frac{1}{4}}$ ) and the quantity  $\kappa$ , are taken as 0.4, 0 and 1 respectively.

$$\text{Consequently, } \Lambda_{LE} = 3.14^\circ$$

$$\text{Hence, } C_{L\alpha} = \frac{2\pi \times 7.8}{2 + \sqrt{\frac{7.8^2 \times 0.936^2}{1} + 4}} = 5.121 \text{ rad}^{-1}$$

From Ref.3.14, chapter 6, the leading edge radius, as a fraction of chord, for NACA 23012 airfoil is :

$$1.109 t^2 = 1.019 \times 0.12^2 = 0.016$$

$$R_{le} = 0.016 \times \bar{c} = 0.016 \times 2.566 = 0.041 \text{ m}$$

Reynolds number, based leading edge radius ( $R_{eLER}$ ), is :

$$R_{eLER} = \frac{0.041 \times 119.5}{14 \times 10^{-6}} = 3.35 \times 10^5$$

$$\begin{aligned} \text{Hence, } R_{eLER} \cot \Lambda_{LE} \sqrt{1-M^2} \cos \Lambda_{LE} &= 3.35 \times 10^5 \times 18.22 \times \sqrt{1-0.351^2} \times 0.998 \\ &= 57.16 \times 10^5 \end{aligned}$$

$$\text{Further, } \frac{A\lambda}{\cos \Lambda_{LE}} = \frac{7.8 \times 0.4}{0.998} = 3.13$$

Flight dynamics-I  
Chapter-3

Corresponding to the above values of  $(R_{eLER} \cot \Lambda_{LE} \sqrt{1-M^2 \cos \Lambda_{LE}})$  and

$(\frac{A\lambda}{\cos \Lambda_{LE}})$ , Fig 3.14 of Ref.3.6, gives  $R = 0.95$ .

Hence,

$$e_{wing} = \frac{1.1 \times 5.121/7.8}{0.95 \times (5.121/7.8) + 0.05 \times \pi} = 0.925$$

To obtain  $e_{fuselage}$ , it is assumed that the fuselage has a round cross section.

In this case, Fig.2.5 of Ref 3.6 gives:  $(\frac{1}{e_{fuselage}}) / (S_{fuselage}/S) = 0.75$  when  $A = 7.8$ .

Consequently,

$$\frac{1}{e_{fuselage}} = 0.75 \times 3.72/51.22 = 0.054$$

$\frac{1}{e_{others}}$  is recommended as 0.05(Ref.3.6, section 2.2)

$$\text{Thus, } \frac{1}{e} = \frac{1}{e_{wing}} + \frac{1}{e_{fuselage}} + \frac{1}{e_{other}} = \frac{1}{0.925} + 0.054 + 0.05 = 1.185$$

$$\text{Or } e = 0.844$$

$$\text{Hence, } \frac{1}{\pi Ae} = \frac{1}{\pi \times 7.8 \times 0.844} = 0.0484$$

Hence, a rough estimate of the drag polar is:

$$C_D = 0.0216 + 0.0484 C_L^2$$

Answer: A rough estimate of the drag polar is :  $C_D = 0.0216 + 0.0484 C_L^2$

**Remark:**

- i) A detailed estimation of the drag polar of Piper Cherokee airplane is presented in appendix A.

**3.2.19 Note on estimation of minimum drag coefficients of wings and bodies**

Remark (ii) of section 3.2.17 mentions that the parasite drag coefficient of an airplane ( $C_{D0}$ ) is given by :

Flight dynamics-I  
Chapter-3

$$C_{D0} = \left( \frac{1}{S} \sum C_{D\pi} S_{\pi} \right) + C_{Dint}$$

where the values of  $C_{D\pi}$  represent the minimum drag coefficients of various components of the airplane.

In example 3.3 the minimum drag coefficients of wing, fuselage, nacelle, horizontal tail and vertical tail were estimated using experimental data. However, the minimum drag coefficients of shapes like the wing, the horizontal tail, the vertical tail and the streamlined bodies can be estimated using the background presented in subsections 3.2.5 to 3.2.10. The procedure for such estimation are available in Ref.3.6 which in turn is based on Ref.3.5. The basis of this procedure is that the minimum drag coefficient of a streamlined shape can be taken as the skin friction drag coefficient of a flat plate of appropriate characteristic length, roughness and area.

With these aspects in view, the procedure to estimate the minimum drag coefficient of the wing can be summarised as follows. It is also illustrated in the sections on drag polar in Appendices A & B.

(a) The reference length ( $l$ ) is the mean aerodynamic chord of the exposed wing i.e. the portion of wing outside the fuselage. This chord is denoted by  $\bar{c}_e$ . Obtain roughness parameter ( $l/k$ ) with  $\bar{c}_e$  as ' $l$ ' and value of  $k$  from Table 3.3.

(b) The flow is assumed to be turbulent over the entire wing.

(c) Choose the flight condition. Generally this is the cruising speed ( $V_{cr}$ ) and the cruising altitude ( $h_{cr}$ ). Obtain the Reynolds number ( $Re$ ) based on  $V_{cr}$ , kinematic

viscosity ( $\nu_{cr}$ ) at  $h_{cr}$  and the reference length as  $\bar{c}_e$  i.e.  $Re = \frac{\bar{c}_e V_{cr}}{\nu_{cr}}$ .

Obtain  $(Re)_{cutoff}$  corresponding to  $(l/k)$  using Fig.3.2 of Ref.3.6. Obtain  $C_{df}$  corresponding to lower of  $Re$  and  $(Re)_{cut-off}$ . Following Ref.3.6 this value is denoted by  $C_{fw}$  in Appendices A & B.

(d) Apply correction to  $C_{fw}$  for type of airfoil and its thickness ratio. Multiply this value by  $(S_{wet}/S_{ref})$ , where  $S_{wet}$  is the wetted area of the exposed wing and  $S_{ref}$  is the reference area of the wing. Refer to section 3.1 of Ref.3.6 for estimation of

Flight dynamics-I  
Chapter-3

$S_{wet}$  and correction for airfoil shape. When the shape of the airfoil changes along the wingspan, a representative section is taken for estimation of  $S_{wet}$ .

Similar procedure can be used to estimate the minimum drag coefficients of the horizontal tail and vertical tail.

As regards estimation of the minimum drag coefficient of fuselage, the reference length is taken as the length of fuselage ( $l_f$ ) and the roughness factor is taken as ( $l_f/k$ ). Correction is applied for fineness ratio ( $l_f/d_e$ ) of the fuselage. Where 'd<sub>e</sub>' is the equivalent diameter of the fuselage (see section 3.2.15). The wetted area in this case is the wetted area of the fuselage.

Finally, correction is applied for wing-body interference effect (see Appendices A & B for details).

Similar procedure can be used to estimate the minimum drag coefficients of bodies like nacelle, external fuel tanks, bombs etc.

**3.2.20 Typical values of  $C_{D0}$ , A, e and subsonic drag polar.**

Based on the data in Ref.3.9, chapter 4 , Ref.3.18 vol. VI , chapter 5 and Ref.3.15 , chapter 6, the typical values of  $C_{D0}$  , A, e and the drag polar for subsonic airplanes are given in Table 3.4.

Type of airplane	$C_{D0}$	A	e	Typical polar
Low speed (M <0.3)	0.025 to 0.04	6 to 8	0.75 to 0.85	$0.025 + 0.06C_L^2$
Medium speed (M around 0.5)	0.02 to 0.024	10 to 12	0.75 to 0.85	$0.022 + 0.04C_L^2$
High subsonic (M around 0.8, Swept wing)	0.014 to 0.017	6 to 9	0.65 to 0.75	$0.016 + 0.045C_L^2$

Table 3.4 Typical values of  $C_{D0}$ , A, e and subsonic drag polar

**Remarks:**

(i) Table 3.4 shows that  $C_{D0}$  for low speed airplanes is higher than other airplanes. This is because these airplanes have exposed landing gear, bluff fuselage (see Fig.1.2a) and struts when a high wing configuration is used. The  $C_{D0}$  for high subsonic airplanes is low due to smooth surfaces, thin wings and slender fuselage. It may be added that during the design process, the values of airfoil thickness ratio, aspect ratio and angle of sweep for the wing are obtained from considerations of optimum performance.

(ii) The low speed airplanes have a value of  $K (=1/\pi Ae)$  higher than the other airplanes. One of the reasons for this is that these airplanes have only a moderate aspect ratio (6 to 8) so that the wing-span is not large and the hanger-space needed for parking the plane is not excessive.

(iii) See section 2 of Appendix A for estimation of the drag polar of a subsonic airplane in cruise and take-off conditions.

**3.2.21 Winglets and their effect on induced drag**

According to Ref.2.1, a Winglet is an upturned wing tip or added axial airfoil above and / or below the wing tips. Figure 1.2c shows one type of winglets at wing tips. The winglets alter the spanwise distribution of lift and reduce the induced drag. Reference 1.9, chapter 4 can be referred for a simplified analysis of the effect of winglets. However, along with reduction in induced drag, the winglets increase the weight of the wing and also the parasite drag. After trade-off studies which take into account the favourable and unfavourable effects of the winglets, the following approximate dimensions are arrived at for the winglets. Root chord of about  $0.65 c_t$ , tip chord of about  $0.2 c_t$  and height of about  $c_t$ ; where  $c_t$  is the tip chord of the wing. As regards the effect on induced drag, Ref.3.15, chapter 5 suggest that the effect of winglets can be approximately accounted for by increasing the wing span by an amount equal to half the height of the winglet. The procedure is illustrated in example 3.4

**Example 3.4**

Consider a wing, with the following features. Area (S) = 111.63 m<sup>2</sup>, Aspect ratio (A) = 9.3, span (b) = 32.22 m, root chord ( $c_r$ ) = 5.59 m,



Flight dynamics-I  
Chapter-3

tip chord ( $c_t$ ) = 1.34 m

Further, the airplane has (a) parasite drag coefficient ( $C_{D0}$ ) = 0.0159 ; (b) Oswald efficiency factor ( $e$ ) = 0.8064 (c) lift coefficient during cruise ( $C_{Lcr}$ )=0.512.

Examine the benefits of fitting winglets to this wing.

**Solution :**

The drag polar of the existing airplane is :

$$C_D = 0.0159 + \frac{1}{\pi \times 9.3 \times 0.8064} C_L^2 = 0.0159 + 0.04244 C_L^2$$

$$\text{When } C_L = 0.512, C_D = 0.0159 + 0.04244 \times 0.512^2 = 0.02703$$

With winglets, the wing span effectively increases to :

$$b_e = b + \frac{c_t}{2} = 32.22 + \frac{1.34}{2} = 32.89 \text{ m}$$

$$\text{Hence, the effective aspect ratio } (A_e) = \frac{b_e^2}{S} = \frac{32.89^2}{111.63} = 9.691$$

Consequently, the drag polar approximately changes to :

$$0.0159 + \frac{1}{\pi \times 9.691 \times 0.8064} C_L^2 = 0.0159 + 0.0407 C_L^2$$

At  $C_L = 0.512$ , the  $C_D$  of the wing with winglet is :

$$0.0159 + 0.04074 \times 0.512^2 = 0.02658$$

Reduction in drag coefficient is  $0.02703 - 0.02658 = 0.00045$  or 1.7%

**Note :**

$$(C_L/C_D)_{\text{existing wing}} = 0.512/0.02703 = 18.94$$

$$(C_L/C_D)_{\text{modified wing}} = 0.512/0.02658 = 19.26$$

### 3.3 Drag polar at high subsonic, transonic and supersonic speeds

At this stage, the reader is advised to revise background on compressible aerodynamics and gas dynamics. References.1.9 & 1.10 may be consulted. Before discussing the drag polar at high subsonic, transonic and supersonic speeds, the relevant features of supersonic and transonic flows are briefly recapitulated in the following subsections.

### 3.3.1 Some aspects of supersonic flow – shock wave, expansion fan and bow shock

When the free stream Mach number roughly exceeds a value of 0.3, the changes in the fluid density, within the flow field, become significant and the flow needs to be treated as compressible. In a compressible flow, the changes of temperature in the flow field may be large and hence the speed of sound ( $a = \sqrt{\gamma RT}$ ) may vary from point to point. When the free stream Mach number exceeds unity, the flow is called supersonic. When a supersonic flow decelerates, shock waves occur. The pressure, temperature, density and Mach number change discontinuously across the shock. The shocks may be normal or oblique. The Mach number behind a normal shock is subsonic; behind an oblique shock it may be subsonic or supersonic. When supersonic flow encounters a concave corner, as shown in Fig.3.22a, the flow changes the direction across a shock. When such a flow encounters a convex corner, as shown in Fig.3.22b, the flow expands across a series of Mach waves called expansion fan. A typical flow past a diamond airfoil at supersonic Mach number is shown in Fig.3.23. If the free stream Mach number is low supersonic (i.e. only slightly higher than unity) and the angle  $\theta$ , as shown in Fig.3.23, is high then instead of the attached shock waves at the leading edge, a bow shock wave may occur ahead of the airfoil. A blunt-nosed airfoil can be thought of an airfoil with large value of ' $\theta$ ' at the leading edge and will have a bow shock at the leading edge as shown in Fig.3.24. Behind a bow shock there is a region of subsonic flow (Fig.3.24).

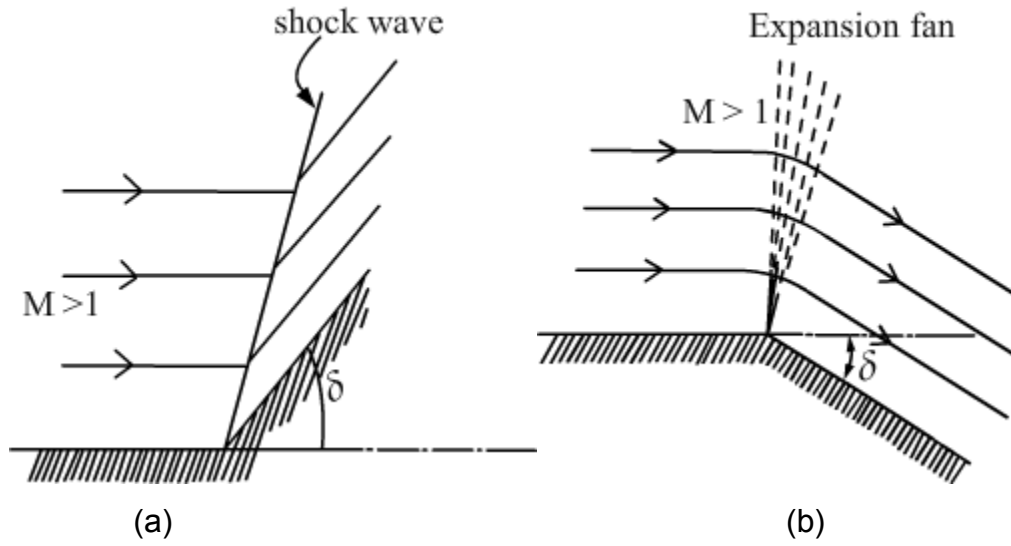


Fig.3.22 Supersonic flow at corners  
(a) Concave corner (b) Convex corner

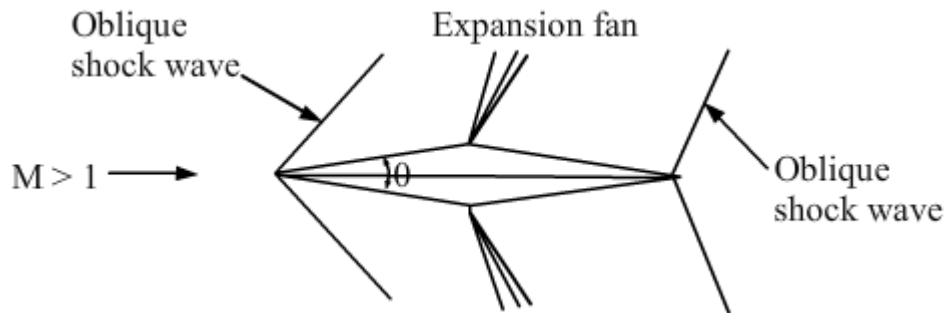


Fig.3.23 Supersonic flow past a diamond airfoil

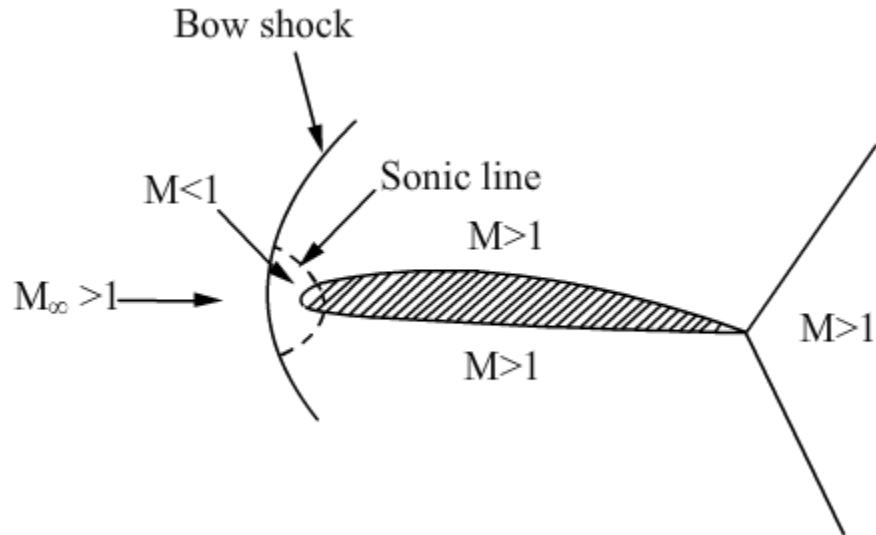


Fig.3.24 Bow shock ahead of blunt-nosed airfoil

### 3.3.2 Drag at supersonic speeds

At supersonic Mach numbers also the drag of a wing can be expressed as sum of the profile drag of the wing section plus the drag due to effect of finite aspect ratio. The profile drag consists of pressure drag plus the skin friction drag. The pressure drag results from the pressure distribution caused by the shock waves and expansion waves (Fig.3.23) and hence is called 'Wave drag'. It is denoted by  $C_{dw}$ . Figures 3.25a and b show the distributions of pressure coefficients ( $C_p$ ) on an airfoil at angles of attack ( $\alpha$ ) of  $0^\circ$  and  $2^\circ$ .

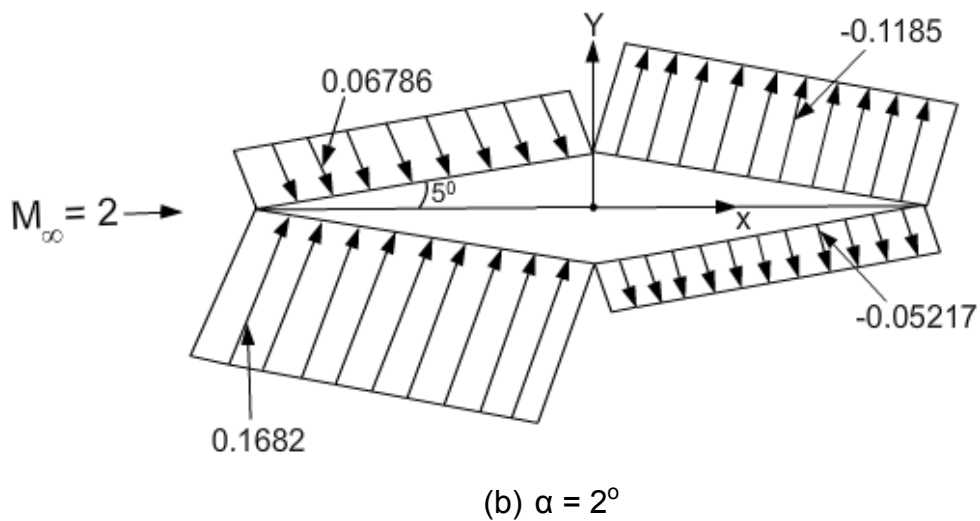
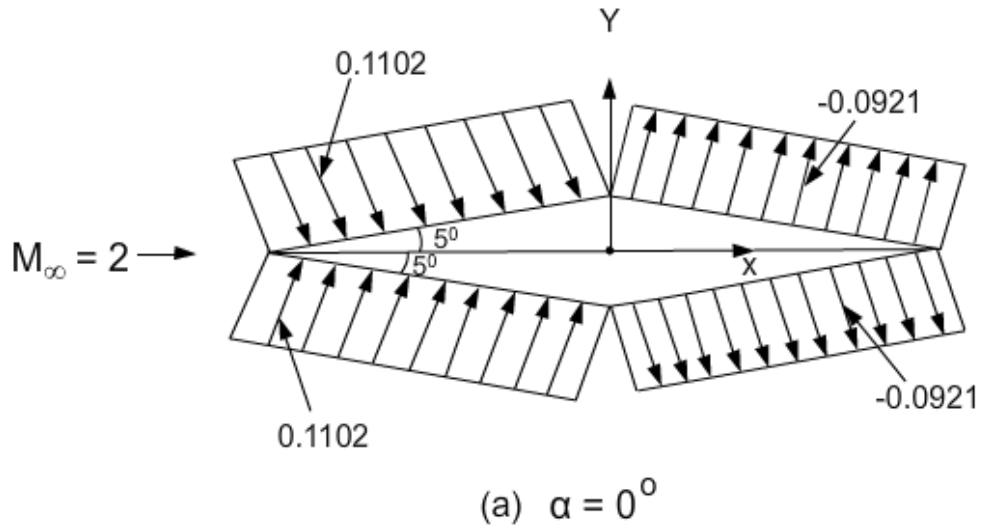


Fig.3.25 Pressure distributions over a diamond airfoil (a)  $\alpha = 0^\circ$  (b)  $\alpha = 2^\circ$

From the distributions of  $C_p$  at  $\alpha = 0^\circ$ , on various faces of the diamond airfoil, it is observed that the distributions are symmetric about the X-axis but not symmetric about the Y-axis. This indicates  $C_l = 0$  but  $C_{dw} > 0$ . From the distributions of  $C_p$  at  $\alpha = 2^\circ$ , it is seen that the distributions are unsymmetric about both X- and

## Flight dynamics-I

### Chapter-3

Y-axes. Thus in this case,  $C_l > 0$  and  $C_{dw} > 0$ . It may be added that a leading edge total angle of  $10^\circ$  would give a thickness ratio of 8.75%, which is rather high. Supersonic airfoils would have  $(t/c)$  between 3 to 5%.

At supersonic speed the skin friction drag is only a small fraction of the wave drag. The wave drag of a symmetrical airfoil ( $C_{dw}$ ) can be expressed as (Ref.1.9, chapter 5):

$$C_{dw} = \frac{4}{\sqrt{M_\infty^2 - 1}} [\alpha^2 + (t/c)^2] \quad (3.48)$$

where  $\alpha$  = angle of attack in radians and

$t / c$  = thickness ratio of the airfoil

The wave drag of a finite wing at supersonic speeds can also be expressed as  $K C_L^2$  (refer Ref.1.9, chapter 5 for details). However, in this case  $K$  depends on the free stream Mach number ( $M_\infty$ ), aspect ratio and leading edge sweep of the wing (refer Ref.1.9 chapter 5 for details).

The estimation of the wave drag of a fuselage at supersonic speeds is more involved than that of the wing. It is considered as flow past a combination of a nose cone, a cylindrical mid-body and a conical after body. It may be added that the supersonic airplanes generally have low aspect ratio wings and the wave drag of the wing-body is analysed as a combination. Reference 1.9, chapter 5 deals with some of these aspects. Reference 3.5 is generally used to estimate the drag of wing-body-tail combination at desired values of Mach numbers.

### 3.3.3 Transonic flow regime, critical Mach number and drag divergence

#### Mach number of airfoil , wing and fuselage

A transonic flow occurs when the free stream Mach number is around one. The changes in the flow and hence in the drag occurring in this range of Mach numbers can be better understood from the following statements.

1) In the subsonic flow past an airfoil the flow velocity is zero at the stagnation point. Subsequently, the flow accelerates, it reaches a maximum value ( $V_{max}$ ) and later attains the free stream velocity ( $V_\infty$ ). The ratio ( $V_{max} / V_\infty$ ) is greater than unity and depends on (a) the shape of airfoil (b) the thickness ratio ( $t/c$ ) and

Flight dynamics-I  
Chapter-3

( c ) the angle of attack ( $\alpha$ ). As  $(V_{\max} / V_{\infty})$  is greater than unity, the ratio of the maximum Mach number on the airfoil ( $M_{\max}$ ) and free stream Mach number ( $M_{\infty}$ ) would also be more than unity. However,  $(M_{\max} / M_{\infty})$  would not be equal to  $(V_{\max} / V_{\infty})$  as the speed of sound varies from point to point in the flow.

II) Critical Mach number: As  $M_{\infty}$  increases,  $M_{\max}$  also increases. The free stream Mach number for which the maximum Mach number on the airfoil equals unity is called the critical Mach number ( $M_{\text{crit}}$ ).

III) The changes in flow patterns when the free stream Mach number changes from subcritical (i.e.  $M_{\infty} \leq M_{\text{crit}}$ ) to supersonic ( $M_{\infty} > 1$ ) are highlighted below .

(A) When  $M_{\infty}$  is less than or equal to  $M_{\text{crit}}$  then the flow is subsonic everywhere i.e. in the free stream, on the airfoil and behind it (Fig.3.26a).

(B) When  $M_{\infty}$  exceeds  $M_{\text{crit}}$ , a region of supersonic flow occurs which is terminated by a shock wave. The changes in flow pattern are shown in Figs.3.26b and c.

(C) As free stream Mach number increases further the region of supersonic flow enlarges and this region occurs on both the upper and lower surfaces of the airfoil (Figs.3.26c, d & e).

(D) At a free stream Mach number slightly higher than unity, a bow shock is seen near the leading edge of the airfoil (Fig.3.26f).

(E) At a still higher Mach numbers, the bow shock approaches the leading edge and if the leading edge is sharp, then the shock waves attach to the leading edge as shown in Fig.3.23.



Fig.3.26 (a) Mach number subsonic everywhere

Flight dynamics-I  
Chapter-3



Fig.3.26 (b)  $M_{\infty}$  only slightly higher than  $M_{crit}$ ; shock waves are not discernible

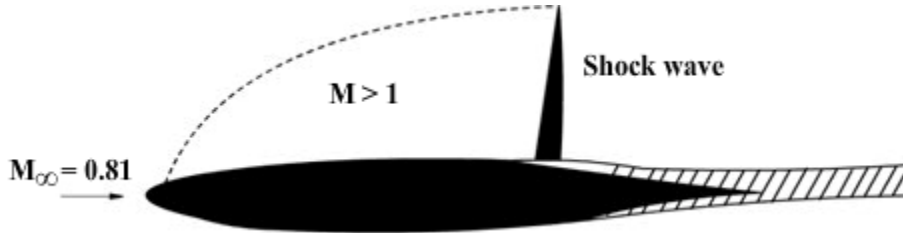


Fig.3.26 (c)  $M_{\infty}$  greater than  $M_{crit}$ ; shock wave seen on the upper surface

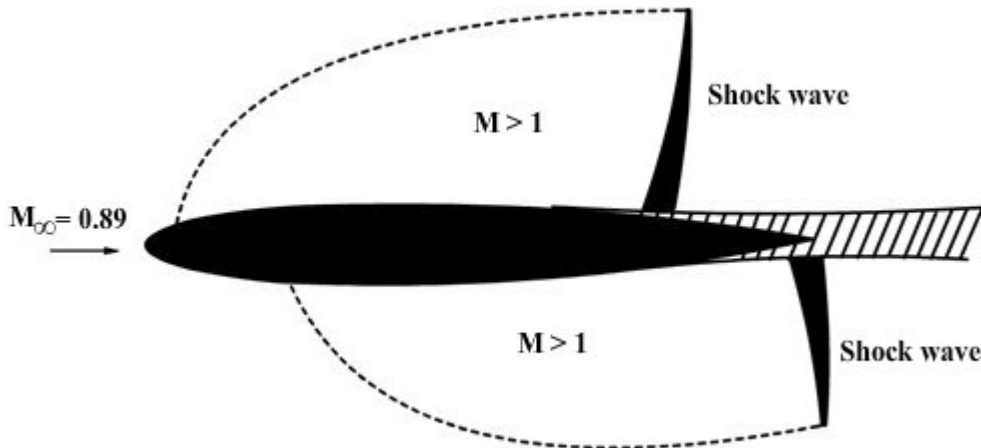


Fig.3.26 (d)  $M_{\infty}$  greater than  $M_{crit}$ ; shock waves seen on both the upper and lower surfaces



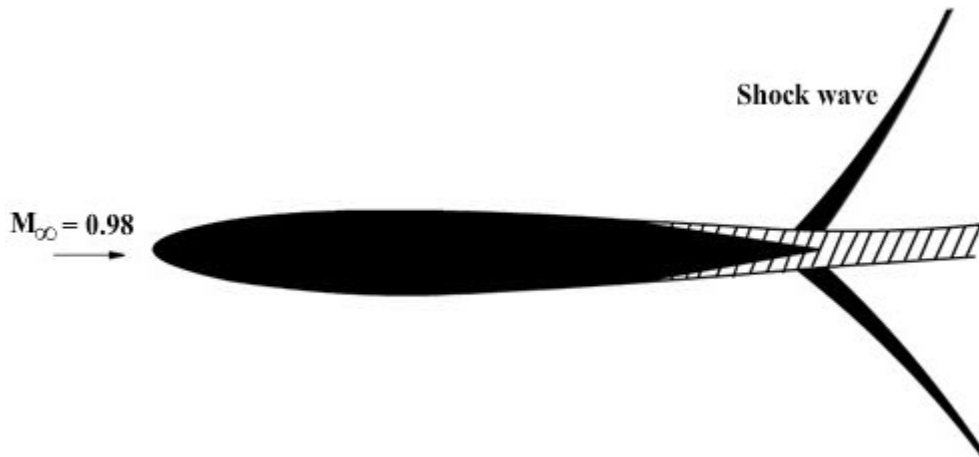


Fig.3.26 (e)  $M_\infty$  greater than  $M_{crit}$ ; shock waves seen on both the upper and lower surfaces at the trailing edge

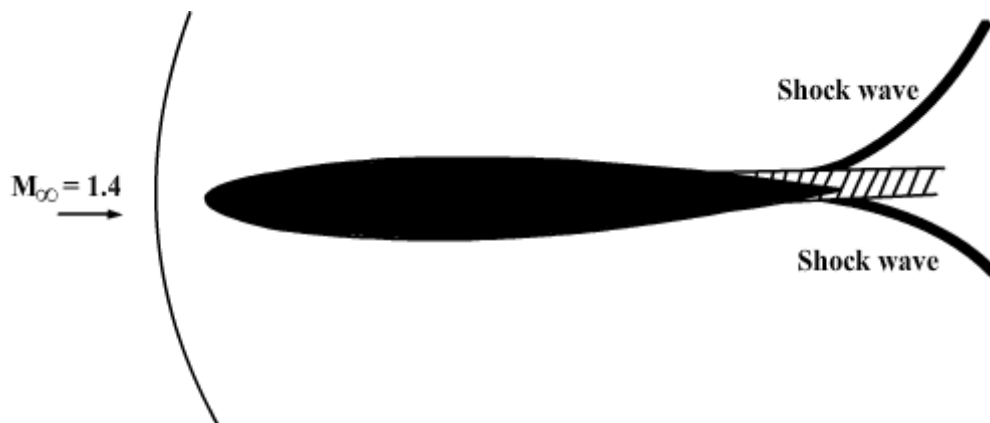


Fig.3.26 (f)  $M_\infty$  greater than unity; bow shock wave seen ahead of the airfoil; shock waves also seen at the trailing edge on both upper and lower surfaces

Fig.3.26 Flow past airfoil in transonic range at  $\alpha=2^\circ$

(Adapted from Ref.3.16, chapter 9 with permission from author). The angle of attack ( $\alpha$ ) being  $2^\circ$  is mentioned in Ref.3.17 chapter 4.

#### (IV) Transonic flow regime

When  $M_\infty$  is less than  $M_{crit}$  the flow everywhere i.e. in the free stream, and on the body and behind it, is subsonic. It is seen that when  $M_{crit} < M_\infty < 1$ ,

## Flight dynamics-I

### Chapter-3

the free stream Mach number is subsonic but there are regions of supersonic flow on the airfoil (Figs.3.26c, d & e). Further, when  $M_\infty$  is slightly more than unity i.e. free stream is supersonic; there is bow shock ahead of the airfoil resulting in subsonic flow near the leading edge (Fig.3.24). When the shock waves are attached to the leading edge (Fig.3.23) the flow is supersonic everywhere i.e. in the free stream and on the airfoil and behind it.

Based on the above features, the flow can be classified into three regimes.

- (a) Sub-critical regime - when the Mach number is subsonic in the free stream as well as on the body ( $M_\infty < M_{crit}$ ).
- (b) Transonic regime - when the regions of both subsonic and supersonic flow are seen within the flow field.
- (c) Supersonic regime - when the Mach number in the free stream as well as on the body is supersonic.

The extent of the transonic regime is commonly stated as between 0.8 to 1.2. However, the actual extent of this regime is between  $M_{crit}$  and the Mach number at which the flow becomes supersonic everywhere. The extent depends on the shape of the airfoil and the angle of attack. In the transonic regime the lift coefficient and drag coefficient undergo rapid changes with Mach number (Figs.3.27a, b and c). It may be recalled that  $C_d$  and  $C_l$  refer to the drag coefficient and lift coefficient of an airfoil respectively.

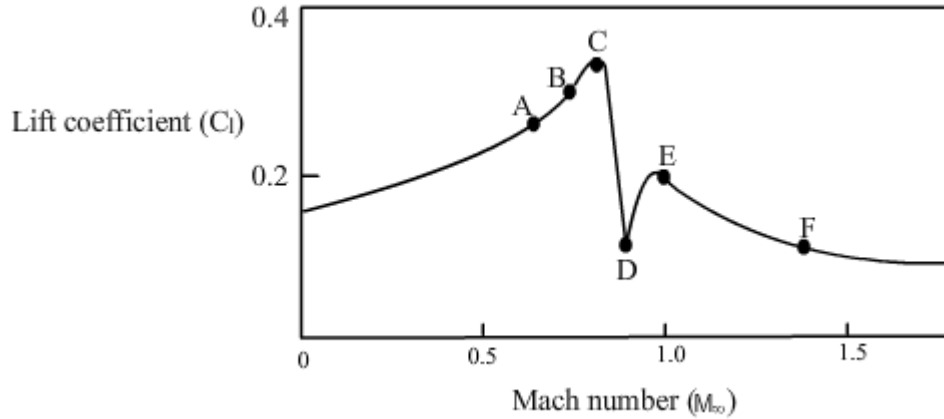


Fig.3.27a Variation of lift coefficient ( $C_l$ ) in transonic range for the airfoil in Fig.3.26 ( $\alpha=2^\circ$ ). (Adapted from Ref. 3.16, chapter 9 with permission from author)  
Note: The points A, B, C, D, E and F corresponds to those in Figs.3.26a, b, c, d, e and f respectively.

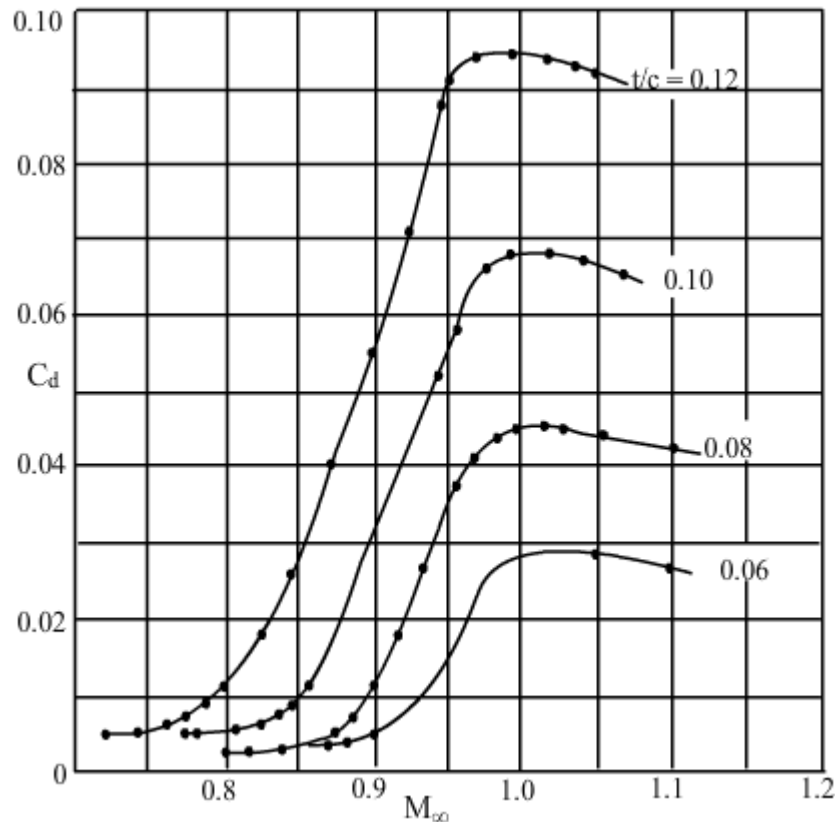


Fig.3.27b Typical variations of drag coefficient ( $C_d$ ) in transonic region for airfoils of different thickness ratios (Adapted from Ref.3.17, chapter 4 with, permission of McGraw-Hill book company)

## Flight dynamics-I

### Chapter-3

Figure 3.27a shows the variation of the lift coefficient ( $C_l$ ) with Mach number at a constant value of angle of attack. It is seen that at sub critical Mach numbers,  $C_l$  increases with Mach number. This is due to the effect of compressibility on pressure distribution. However, as the critical Mach number is exceeded the formation of shocks changes the pressure distributions on the upper and lower surfaces of the airfoil and the lift coefficient decreases (points C & D in Fig.3.27a). This phenomenon of decrease in lift due to formation of shocks is called 'Shock stall'. For a chosen angle of attack the drag coefficient begins to increase near  $M_{crit}$  and reaches a peak around  $M_\infty = 1$  (Fig.3.27b).

#### (V) Drag divergence Mach number ( $M_D$ )

The critical Mach number ( $M_{crit}$ ) of an airfoil has been defined in statement (II) of this subsection. It is the free stream Mach number ( $M_\infty$ ) for which the maximum Mach number on the airfoil equals one. The critical Mach number is a theoretical concept. It is not possible to observe this ( $M_{crit}$ ) in experiments as the changes in flow, when  $M_\infty$  just exceeds  $M_{crit}$ , are very gradual. Hence, a Mach number called 'Drag divergence Mach number ( $M_D$ )' is used in experimental work. The basis is as follows.

When the change in  $C_D$  with Mach number is studied experimentally, the effects of changes in flow, due to the appearance of shock waves, are noticed in the form of a gradual increase in the drag coefficient. The Mach number at which the increase in the drag coefficient is 0.002 over the value of  $C_D$  at sub-critical Mach numbers is called 'Drag divergence Mach number' and is denoted by  $M_D$ .

Figure 3.27c shows a typical variation of  $C_D$  with  $M$  and also indicates  $M_D$ .

The following may be added. (a) For a chosen angle of attack the value of  $C_D$  remains almost constant when the Mach number is sub-critical. (b) The drag divergence Mach number of an airfoil depends on its shape, thickness ratio and the angle of attack. (c) The increase in the drag coefficient in the transonic region

Flight dynamics-I  
Chapter-3

is due to the appearance of shock waves. Hence, this increment in  $C_d$  is called wave drag.

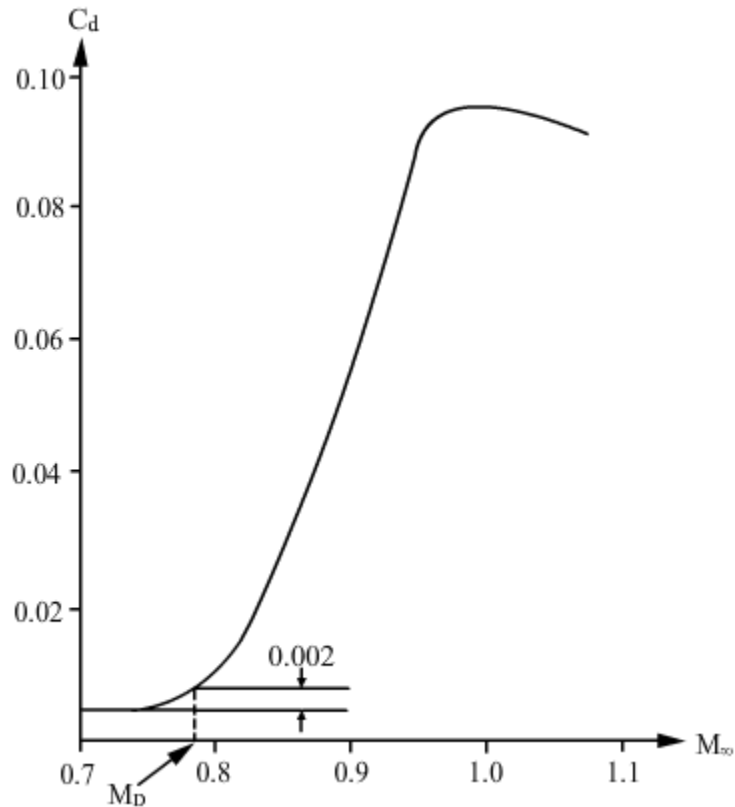


Fig.3.27c Definition of drag divergence Mach number  
(The curve corresponds to  $t/c = 0.12$  in Fig.3.27b)

**Remark:**

**Supercritical airfoil**

For airplanes flying at high subsonic speeds the lift coefficient under cruising condition ( $C_{Lcr}$ ) is around 0.5. At this value of lift coefficient, the older NACA airfoils have drag divergence Mach number ( $M_D$ ) of around 0.68 for a thickness ratio ( $t/c$ ) of around 15%.

With the advancements in computational fluid dynamics (CFD) it was possible, in 1970's to compute transonic flow past airfoils. This enabled design of improved airfoils, called supercritical airfoils, which have  $M_D$  around 0.75 for  $t/c$  of 15% (Ref.3.18 part II, chapter 6). For comparison, the shapes of older airfoil (NACA 66<sub>2</sub> – 215) and a supercritical airfoil are shown in Fig.3.20d and f. Note

the flat upper surface of the supercritical airfoil (refer Ref. 1.9 chapter 3 for additional information).

### (VI) Drag divergence Mach number of a wing

The drag divergence Mach number of an unswept wing depends on the drag divergence Mach number of the airfoil used on the wing and its aspect ratio. The drag divergence Mach number of the wing can be further increased by incorporating sweep ( $\Lambda$ ) in the wing. Figure 3.3 shows the geometrical parameters of the wing including the sweep. The beneficial effects of sweep on (a) increasing  $M_D$ , (b) decreasing peak value of wave drag coefficient ( $C_{D_{peak}}$ ) and (c) increasing the Mach number, at which  $C_{D_{peak}}$  occurs, are evident from Fig.3.28.

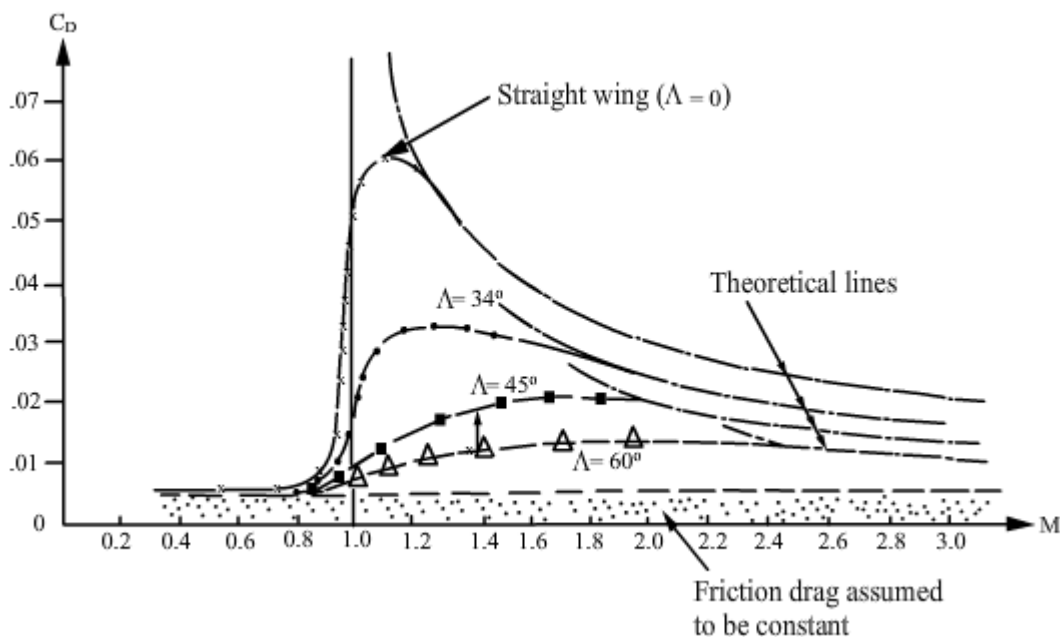


Fig.3.28 Effect of wing sweep on variation of  $C_D$  with Mach number.

(Adapted from Ref.3.3, chapter 16 with permission)

### (VII) Drag divergence Mach number of fuselage

It can be imagined that the flow past a fuselage will also show that the maximum velocity ( $V_{max}$ ) on the fuselage is higher than  $V_\infty$ . Consequently, the

Flight dynamics-I  
Chapter-3

fuselage will also have critical Mach number ( $M_{crit}$ ) and drag divergence Mach number. These Mach numbers depend on the fineness ratio of the fuselage. For the slender fuselage, typical of high subsonic jet airplanes,  $M_{crit}$  could be around 0.9. When  $M_{crit}$  is exceeded the drag of the fuselage will be a function of Mach number in addition to the angle of attack.